Chapter 6
Electrolytic Plasma Treatment of Turkurite-Phase in High-Speed Steels:
High Temperature Testing of Nitrided Layers High-Speed Steel

Zarina Aringozhina
https://orcid.org/0009-0001-8428-4033
D. Serikbayev East Kazakhstan Technical University, Kazakhstan

Yerkezhan Tabiyeva
https://orcid.org/0000-0002-9726-7187
D. Serikbayev East Kazakhstan Technical University, Kazakhstan

Bauyrzhan Rakhadilov
PlasmaScience LLP, Kazakhstan

Waqar Ahmed
University of Lincoln, UK

Didar Yeskermessov
https://orcid.org/0000-0002-2206-8132
D. Serikbayev East Kazakhstan Technical University, Kazakhstan

ABSTRACT

Scanning electron microscopy (SEM), EBSD-analysis, and X-ray structure (XRD) analysis were used to investigate the microstructure, morphology, elemental composition, phase composition, and crystal structure of M2 high speed steel after standard thermal treatment. It has been shown that the microstructure of the M2 high speed steel after hardening and three-time tempering consists of tempered martensite and solid carbide M6C-type and MC spherical shape. The volume fraction of carbides and their distribution have been defined. The main carbides in the study of steel after heat treatment – M6C and MC carbides who have a complex FCC lattice and space group Fd3m, have been established by X-ray structural analysis. Carbides are homogeneous and single crystal. EBSD-analysis method with the support of X-ray structural analysis has established that the bright carbides spherical shape M6C correspond to the composition Fe3W3C, and grey carbides spherical shape MC correspond to the composition of the VC.

DOI: 10.4018/978-1-6684-6830-2.ch006

INTRODUCTION

This study focused on the changes in the structure, phase composition of the surface layers of M2 high speed steels resulting from electrolytic-plasma nitriding treatment. It is well known (Parfenov et al., 2007) that treatment by electrolytic-plasma action causes significant changes in the structural-phase states of the material in thin surface layers occur due to the physical action of low-temperature plasma ions and electric discharge. Structural phase transformations occur under conditions far from thermodynamically equilibrium states and make it possible to obtain modified surface layers with a unique set of physical and mechanical properties (Gupta et al., 2007; Pogrebnjak et al., 2016).

High cutting properties of high-speed steels (high heat resistance in the presence of high hardness and wear resistance) are achieved through special alloying and complex heat treatment with a certain phase composition (Plotnikov et al., 2016). The main alloying elements of high-speed steels are carbon, tungsten, molybdenum, vanadium, and chromium. These elements under certain temperature-time conditions form particles in the steel carbide phase strengthening the material (Suminov,, 2005). This leads to a reduction in the carbon content in martensite and formation of ultramicroscopic carbides. These carbides play an important role in mechanical properties of steel such as hardness, wear resistance and heat resistance. Microstructure analysis, of steel after quenching followed by tempering, can be used to evaluate its properties under operatingconditions. Studies linking the microstructure of a material with its physical and mechanical properties have been carried out widely. However, little work has been done on the carbide phases, which play an important role in mechanical properties of M2 high-speed steel. Therefore, microstructures of high-speed steel and its carbide phases is very important. This study of changes in the structural-phase state of high-speed steels due to electrolytic-plasma nitriding is of significant scientific and practical interest.

MATERIALS, EQUIPMENT, AND RESEARCH METHODS

M2 high-speed steel was used as the material in this study. The use of high-speed steels for cutting tools makes it possible to increase the cutting speed by several times, and tool life by dozens of times (Petrova, 2001). The main distinguishing feature of high-speed steels is their high heat resistance or red hardness (600-700°C) in the presence of high hardness (63-70 HRC) and tool wear resistance. The unique properties of high-speed steels are achieved through special alloying and complex heat treatment, providing a certain phase composition (Moiseev, & Grigor'ev,, 2004). Table 1 shows the chemical composition of M2 high speed steels.

The choice of research materials is also justified by the fact that M2 high-speed steels are common in metalworking, typical high-speed steels of moderate heat resistance. Currently, to reduce the consumption of expensive and scarce elements, especially tungsten, sparingly alloyed steels are used. Of these,

Table 1. Chemical composition of M2 high speed steel (GOST 19265-73)

Grade Steel	C	Mn	Si	Cr	W	V	Co	Mo	Ni	S	P
M2	0.82-0.9	0,20 - 0.50	0,20 - 0.50	3.80 - 4.40	5.50 - 6.50	1.70-2.10	before 0.50	4.80-5.30	before 0.60	before 0.025	before 0.03

M2 steel has the widest application. Blanks of steel samples for research in the form of parallelepipeds with dimensions10×30×30 mm^3 cut out from bars of M2 steel were used. The samples were subjected to standard heat treatment: quenching from 1230°C in oil and subsequent tempering at 560°C three times for a duration of 1 hour each and cooling in the air (Petrova, 2004).

Optical metallography was used to determine the structure. For metallographic analysis, an optical light microscope "ALTAMI-MET-1M" was used. X-ray diffraction studies of steel samples were performed using known methods of XRD on X'PertPRO diffractometers. Diffraction patterns were taken using CuK_α radiation (λ=1.540598 Å) at a voltage of 35 kV. In the D8 ADVANCE diffractometer, reflection from a flat pyrographite monochromator was used in front of the detector to isolate a narrow portion of the spectrum (monochromatization), and K_α radiation with certain wavelengths was selected into the detection unit.The interpretation of the diffraction patterns was carried out manually using standard methods and the PDF-4 database, and the quantitative analysis was performed using the Powder Cell program. The morphology and elemental composition of the sample treated in electrolytic plasma was studied in the engineering laboratory "VERITAS" of the VKTU named after D. Serikbaev on a JSM-6390LV scanning electron microscope - JEOL (Japan), with an INCAEnergy energy-dispersive microanalysis attachment from OXFOR D Instruments. Studies of the phase composition of carbide phases and their sizes were carried out by EBSD analysis (analysis of backscattered electrons) on a system with electron and focused ion beams Quanta 200 3D.

RESULTS AND DISCUSSION OF RESEARCH

To establish the main regularities of structural-phase transformations in high-speed steels during electrolytic-plasma nitriding, the structural-phase states of M2 high speed steel samples of high-speed steels in the initial state were studied.

Figure 1 shows the microstructures of M2 steel i.e. after standard heat treatment. The microstructures of M2 steels consist of tempered martensite and special carbides (Figure1). In previous studies (Skakov, Rakhadilov, and Sheffler, 2013; Skakov, Rakhadilov, and Karipbayeva, 2013), we found that martensite and special carbides are present in the steel structure after standard heat treatment. No residual austenite was observed in the matrix. The preliminary estimate was confirmed by X-ray diffraction phase analysis.

Figure 1. Microstructure of M2 high-speed steel before (a) and after (b) of electrolytic-plasma nitriding

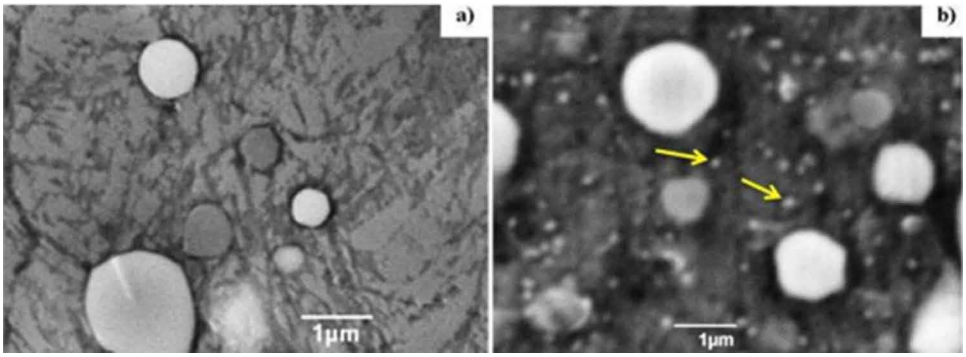

Figure 2. Surface microstructure and distribution map of alloying elements of M2 high speed steel before nitriding

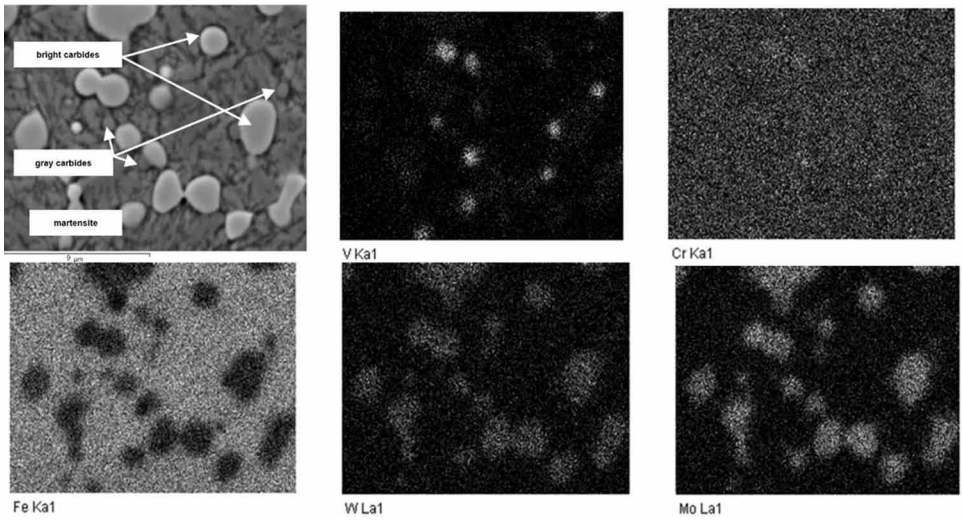

To reveal the composition of carbides and their distribution, a map of the distribution of alloying elements in the steel structure was obtained. The general nature of the distribution of alloying elements in the structure of M2 steels is shown (Figures 1). Light spherical carbides contain tungsten and molybdenum, and gray carbides is enriched with vanadium. The maps of the distribution of alloying elements confirmed that two types of carbides are present in M2 steels - light and dark. It should be kept in mind that V, W, Mo and Cr are carbide-forming elements. The carbides of these metals have a high binding energy and stability (Erkinbekkyzy et al., 2020; Kremnev,, 2008; Skakov, Kurbanbekov, Tabieva et al, 2013; Skakov, Rakhadilov, & Karipbaeva, 2013). Hence, the most of the alloying elements are in carbides, and not in solid solution.

To determine the elemental composition of particles of precipitated carbides and matrix (martensite), microprobe analysis was carried out (Figure 2). Table 1 shows alloying elements in carbides and matrix for steel M2. Tungsten, molybdenum, vanadium, and chromium form special carbides in steel: M_6C based on tungsten and molybdenum, MC (special carbides) based on vanadium and $M_{23}C_6$ based on chromium. The results of mapping and microprobe analysis show that the structure of M2 steel after standard heat treatment contains M_6C and MC carbides and no $M_{23}C_6$ carbides, which is in good agreement with the literature data (Kremnev,, 2008; Vorob'yeva, & Skladnova,, 2003). However, some studies (Guenzel et al., 2000; Ivanov et al., 2002) show that after the standard heat treatment, only M_6C type carbide particles are present in the structure of M2 steel. This could be due to the small volume fraction of particles of MC type carbides and the similarity of these particles with the matrix, which makes it impossible to detect them. The methods used in these works have limitations in the detection of carbide particles with a low concentration. Therefore, in this study, along with X-ray diffraction phase analysis, special methods of scanning electron microscopy are used.

The supposed observed carbide M_6C is between the formulas $Fe_3(W, Mo)_3C$ - $Fe_3(W, Mo)_2C$. In other words, together with tungsten and molybdenum atoms, M_6 carbide can contain up to 2/3 iron atoms out of the total number of metal atoms. In addition, chromium and vanadium atoms can be dissolved,

Table 2. The content of alloying elements in the structural components of high speed steels after heat treatment

Structural Components	Content of Elements, % (wt.)				
	V	Cr	Fe	Mo	W
M2 high speed steel					
Bright carbides	3.42	3.31	30.85	26.05	36.37
Gray carbides	26.47	4.45	30.82	16.62	21.64
Martensite	1.33	4.62	84.50	4.25	5.30

Figure 3. X-ray diffraction patterns of high-speed steels in the initial state (after heat treatment)

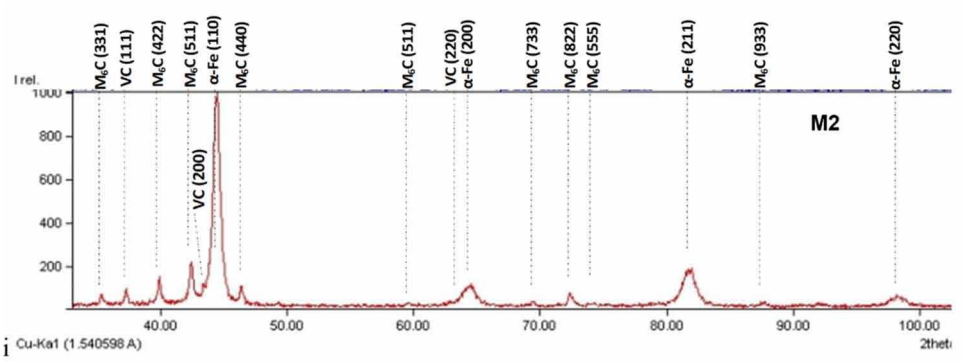

which replace iron atoms. According to the results of microprobe analysis, it can be assumed that the gray carbide particles are vanadium-based MC carbides.

Figure 3 shows the diffraction patterns of M2 steel. XRD analysis showed that in the initial state, i.e., after heat treatment, the structure of M2 steel contains an α-phase and carbides M_6C, MC. Thus, XRD confirmed that the main carbides in the steel samples are M_6C and MC carbides. It has been shown that M_6C type carbides, which have a complex FCC crystal lattice and Fd3m space group, correspond to the Fe_3W_3C composition. The MC type carbides, have a cubic crystal lattice and Fm3m space group, corresponding to the VC (vanadium carbides) composition. In this case, it should benoted that the M_6C type carbide can have both Fe_3W_3C and Fe_3Mo_3C forms. One of the advantages of XRD is that the peak position and lattice parameters can be determined accurately. Nevertheless, when studying individual carbides, it is advisable to apply the EBSD analysis. Therefore, to confirm the results of X-ray diffraction analysis, the crystal structure of M_6C and MC carbides was studied by EBSD analysis using a reflected electron detector on a scanning microscope (system) with electron and focused ion beams.

Figure 4 shows the results of an EBSD analysis of the surface of M2 steel. The EBSD analysis showed that tungsten-rich M_6C carbides are most optimally combined with the Fe_3W_3C cubic phase, while MC-type carbides correspond to the VC phase. However, it is worth noting that in this case Fe_3W_3C other carbide-forming elements are present in the form of M_6C carbides.

In this study we have characterised the structures and carbide phases of M2 high-speed steel in the initial state, i.e. after standard heat treatment. The study of structural-phase states before a certain treatment is necessary in terms of identifying patterns of structure changes and its effect on properties. Since

Figure 4. Results of EBSD analysis of M2 steel

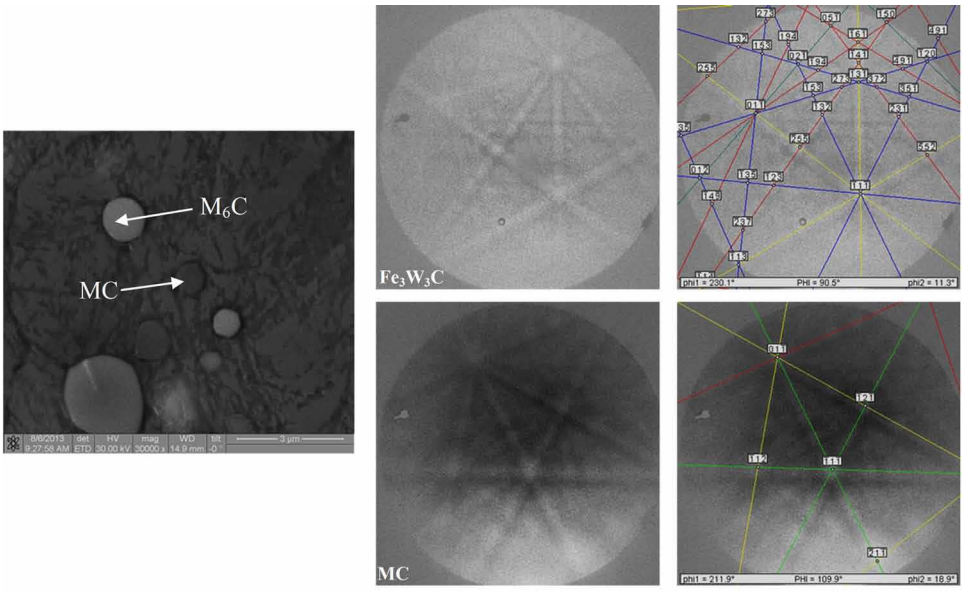

Figure 5. Microstructure of the modified layer of high-speed steels after nitriding a) M2, at 450°C; b) M2, at 500°C; c) M2, at 550°C

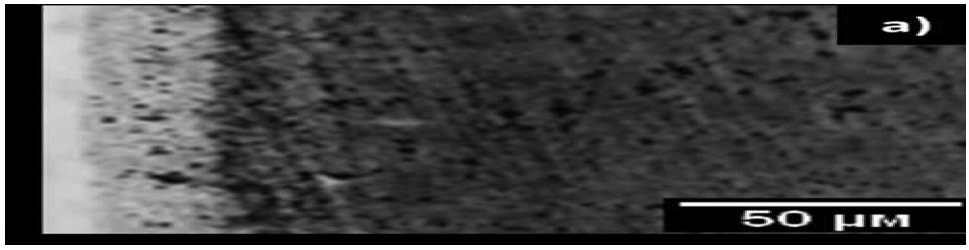

the physical and mechanical properties of high-speed steel are largely determined by the structure and state of the carbide phases and their shape, size, distribution in volume.

Figure 5 shows the microstructures of the modified surface layer of samples of M2 high-speed steels nitrided for 7 minutes. After nitriding, a dark-etched nitrided layer is observed on the surface, which is a zone of internal nitriding. In this case, the dark-etched zone smoothly passes into the base. As expected, after nitriding at temperatures of 450°C, 500°C and 550°C, the thickness of the nitrided layer of M2 steel is 25–40 µm and increases with temperature.

Metallographic analysis has shown that during nitriding by electrolytic-plasma action, diffusion saturation of steel with nitrogen proceeds with accelerated formation of a modified layer consisting only of a well-developed zone of internal nitriding (diffusion layer).

The dependence of the thickness of the diffusion layer of the M2 steel on the exposure time at various nitriding temperatures is evident. Figure 6 shows that the thickness of the modified layer increases with nitriding temperature and holding time. A modified layer is obtained withthe thickness controlled

Figure 6. Growth kinetics of nitrided layers of M2 steel at different temperatures depending on the holding time 1 -450°C; 2 -500°C; 3 -550°C

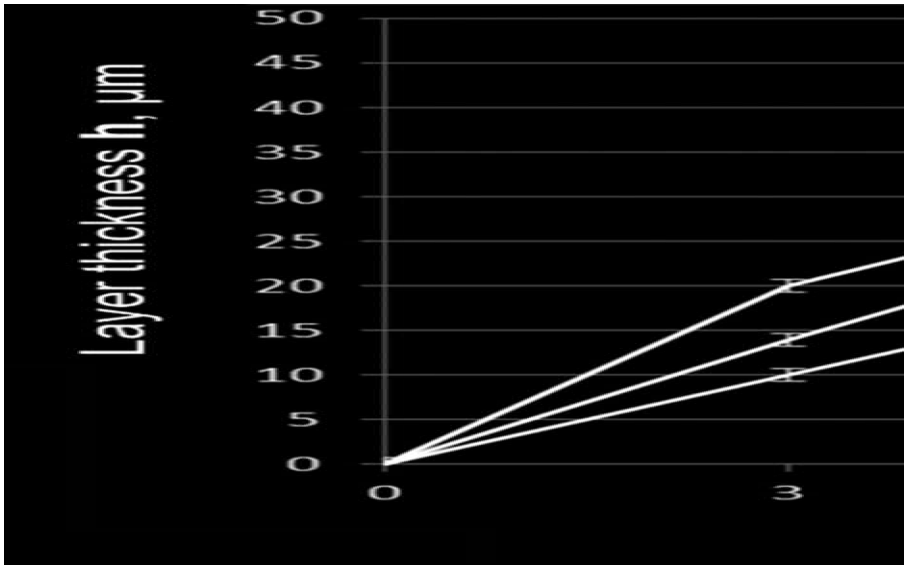

by varying the temperature and nitriding time. Studies (Artinger, 1982; Lakhtin,, 2009), for a cutting tool reveal that the value of h (layer thickness) should not exceed 50–60 μm. Therefore, the modes of nitriding studies are suitable for hardening cutting tools. The optimal time for electrolytic-plasma nitriding for high-speed steel is 7 minutes. Hence, only samples nitride for 7 minutes were studied further.

Figures 7 show SEM images of the surface of M2 steels before and after nitriding for 7 minutes. SEM showed that after electrolytic-plasma nitriding at 550°C, fine particles are formed on the surface of M2 steel (Figure 7 d, fine particles are marked by arrows). And when nitriding at 450°C and 500°C, they are not observed (Figure 7. b, c). The formation of fine nitrides of alloying elements at a temperature of 550°C is possible due to the fact that this temperature corresponds to the tempering temperature of this steel. Since, during the tempering of M2 steel at a temperature of 550–560°C, precipitation hardening occurs as a result of the partial decomposition of martensite and the precipitation of finely dispersed inclusions of strengthening phases (Artinger, 1982).

Figures 8, 9 and 10 show the results of surface mapping of M2 steel after nitriding at 450°C, 500°C and 550°C. The mapping results showed that after nitriding, the surface of M2 steel is saturated with nitrogen. In this case, after nitriding at 500°C and 550°C, areas are observed in the surface where the nitrogen content is higher. These areas are most consistent with the matrix. However, mapping does not allow one to accurately determine which structural component is more saturated with nitrogen, i.e. where nitrides are located. Therefore, to identify the nitrogen content in the structural components and changes in the chemical composition of the surface as a whole, it is necessary to conduct a quantitative energy dispersive analysis of the surface. In order to identify changes in the elemental composition of the surface after nitriding, an energy dispersive analysis of the surface of M2 steel samples nitrided at 450°C, 500°C, and 550°C was carried out.

Figures 11, 12 and 13 show the results of the energy dispersive analysis.

Figure 7. Microstructure of M2 high-speed steel before (a) and after electrolytic-plasma nitriding at temperatures of 450°C (b), 500°C (c), 550°C (d)

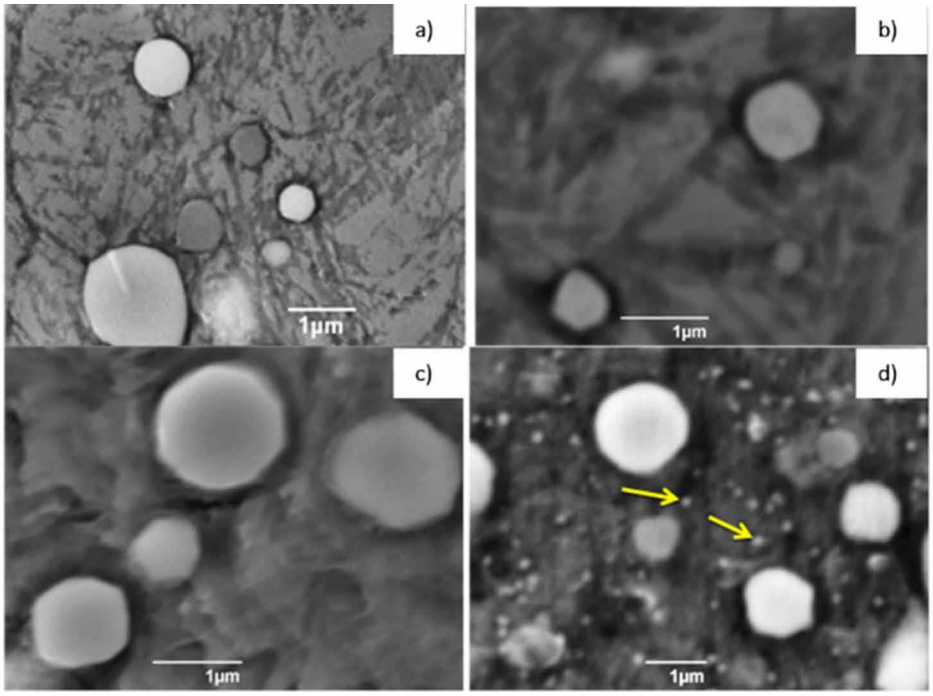

Figure 8. Surface microstructure and distribution map of alloying elements of M2 steel after nitriding at 450°C

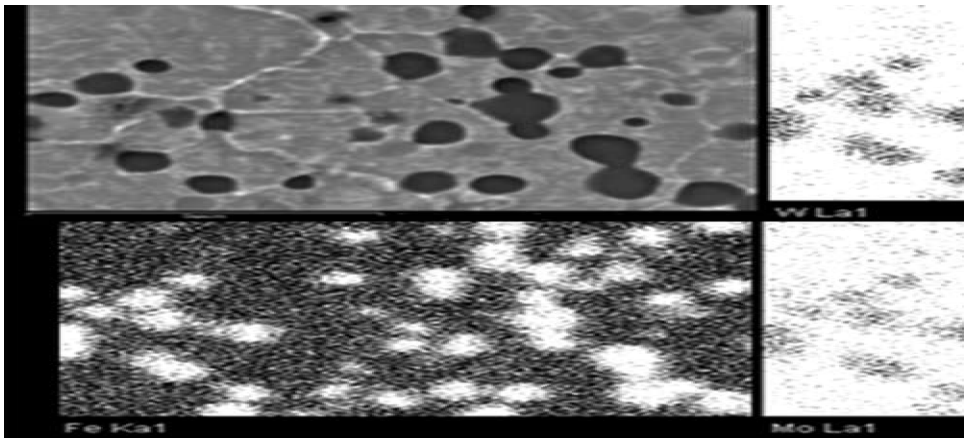

The analysis showed that nitrogen is observed only in the matrix, as expected from the mapping results. The nitrogen content in the surface of M2 steel reaches up to 7% (in weight%). The results of mapping and energy dispersive analysis showed a more uniform distribution of nitrogen over the matrix of the nitrided layer. The observed phenomenon of uniform adsorption and uniform growth of the nitrided layer should be explained by the appearance of a special defective substructure in the grain volume

Figure 9. Surface microstructure and distribution map of alloying elements of M2 steel after nitriding at 500°C

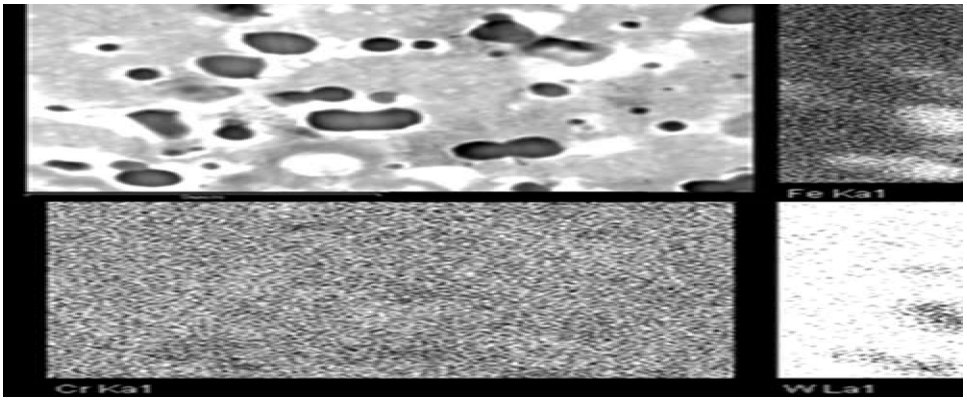

Figure 10. Surface microstructure and distribution map of alloying elements of M2 steel after nitriding at 550°

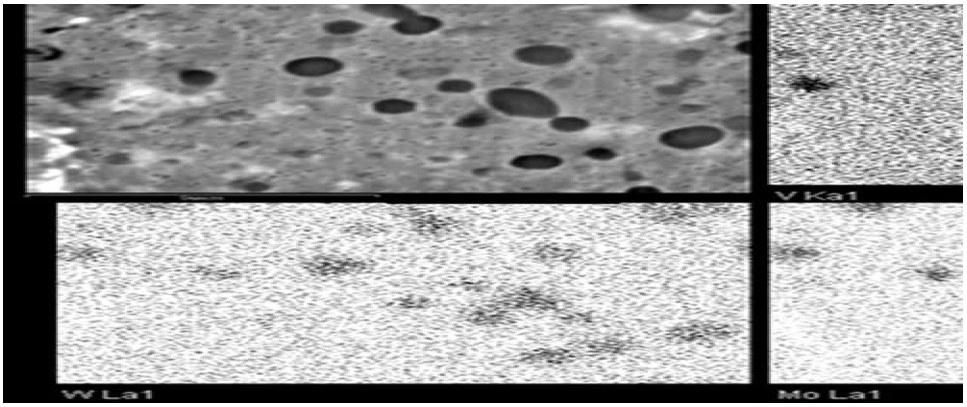

(dislocation-disclination structure of grains in the near-surface zone). The resulting imperfection, apparently, approaches the defectiveness of the grain boundaries. Since, electrolytic-plasma nitriding is carried out under conditions of excessive excitation of the metal surface and subsurface layers. An important factor affecting the growth rate of the nitrided layer and its structure in this process is the exclusion of the predominant role of boundary diffusion. Plasma, accelerating the directed mass transfer of ions to the surface of the sample, creates conditions for the uniform adsorption of nitrogen atoms over the entire surface of the metal, and not selectively along the grain boundaries, as is observed during conventional nitriding by traditional methods.

Thus, the conducted studies have shown that after electrolytic-plasma nitriding, a modified layer is formed on the surface layer of high-speed steels, consisting of a diffusion layer, which is a nitrogenous martensite with fine nitrides of alloying elements. It is determined that the surface is saturated with nitrogen up to 7% (in weight %). Nevertheless, in order to verify the results obtained and to establish the regularities of the formation of the modified layer, it is necessary to study the phase transformations in the surface layers of high-speed steel during nitriding by the X-ray diffraction analysis.

Figure 11. SEM image of M2 steel after nitriding at 450°C (a), characteristic radiation spectra (b) and microanalysis results

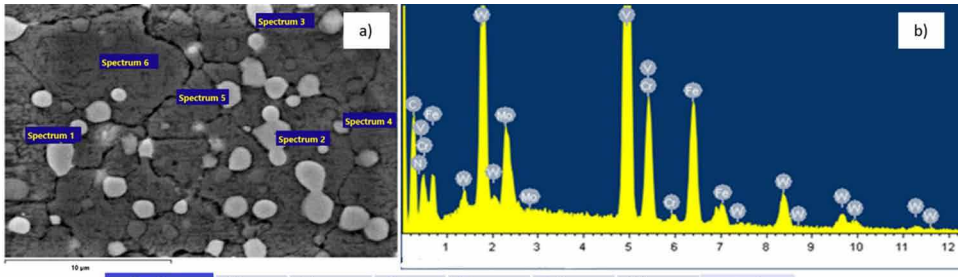

Spectrum	N	V	Cr	Fe	Mo	W	Total
Spectrum 1	0.00	39.66	5.78	17.06	9.87	27.63	100.00
Spectrum 2	0.00	2.31	3.40	26.73	13.74	53.82	100.00
Spectrum 3	0.00	2.42	3.25	26.60	13.55	54.18	100.00
Spectrum 4	0.06	4.06	4.69	78.71	3.33	9.15	100.00
Spectrum 5	0.12	12.33	5.05	65.71	3.91	12.88	100.00
Spectrum 6	0.40	1.03	4.44	85.09	1.97	7.07	100.00

c)

Figure 12. SEM image of M2 steel after nitriding at 500°C (a), characteristic radiation spectra (b) and microanalysis results (c)

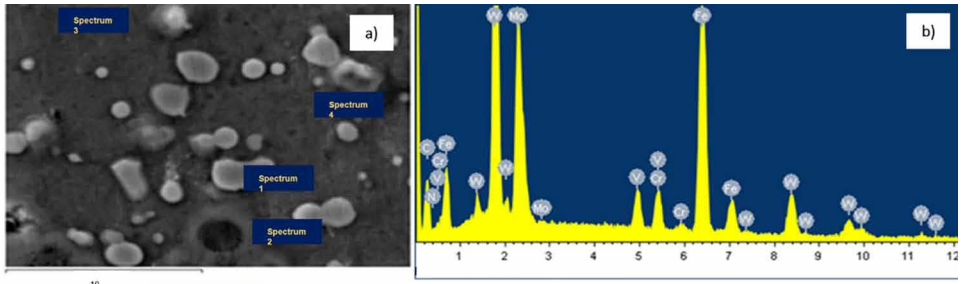

Spectrum	N	V	Cr	Fe	Mo	W	Total
Spectrum 1	0.00	3.25	3.51	32.04	25.91	35.29	100.00
Spectrum 2	6.36	9.86	6.14	62.59	7.12	7.93	100.00
Spectrum 3	5.87	1.45	4.70	80.41	3.60	3.97	100.00
Spectrum 4	6.00	1.56	4.91	78.45	3.97	5.11	100.00

c)

Figure 13. SEM image of M2 steel after nitriding at 550°C (a), characteristic radiation spectra (b) and microanalysis results (c)

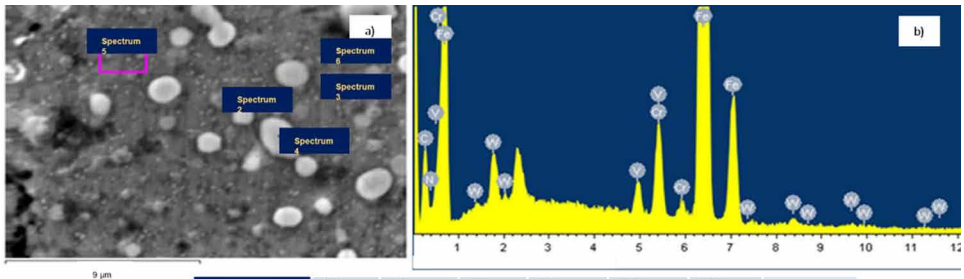

Spectrum	N	V	Cr	Fe	Mo	W	Total
Spectrum 2	0.14	10.46	5.19	72.12	5.29	6.80	100.00
Spectrum 3	7.08	1.82	5.12	77.05	4.47	4.46	100.00
Spectrum 4	0.00	1.47	4.53	33.93	24.26	35.81	100.00
Spectrum 5	5.91	2.47	5.12	78.02	3.94	4.54	100.00
Spectrum 6	3.58	2.59	4.78	81.23	3.21	4.61	100.00

c)

Figure 14. XRD patterns of samples of M2 high-speed steel before (a) and after nitriding at temperatures of 450°C (b), 500°C (c) and 550°C (d)

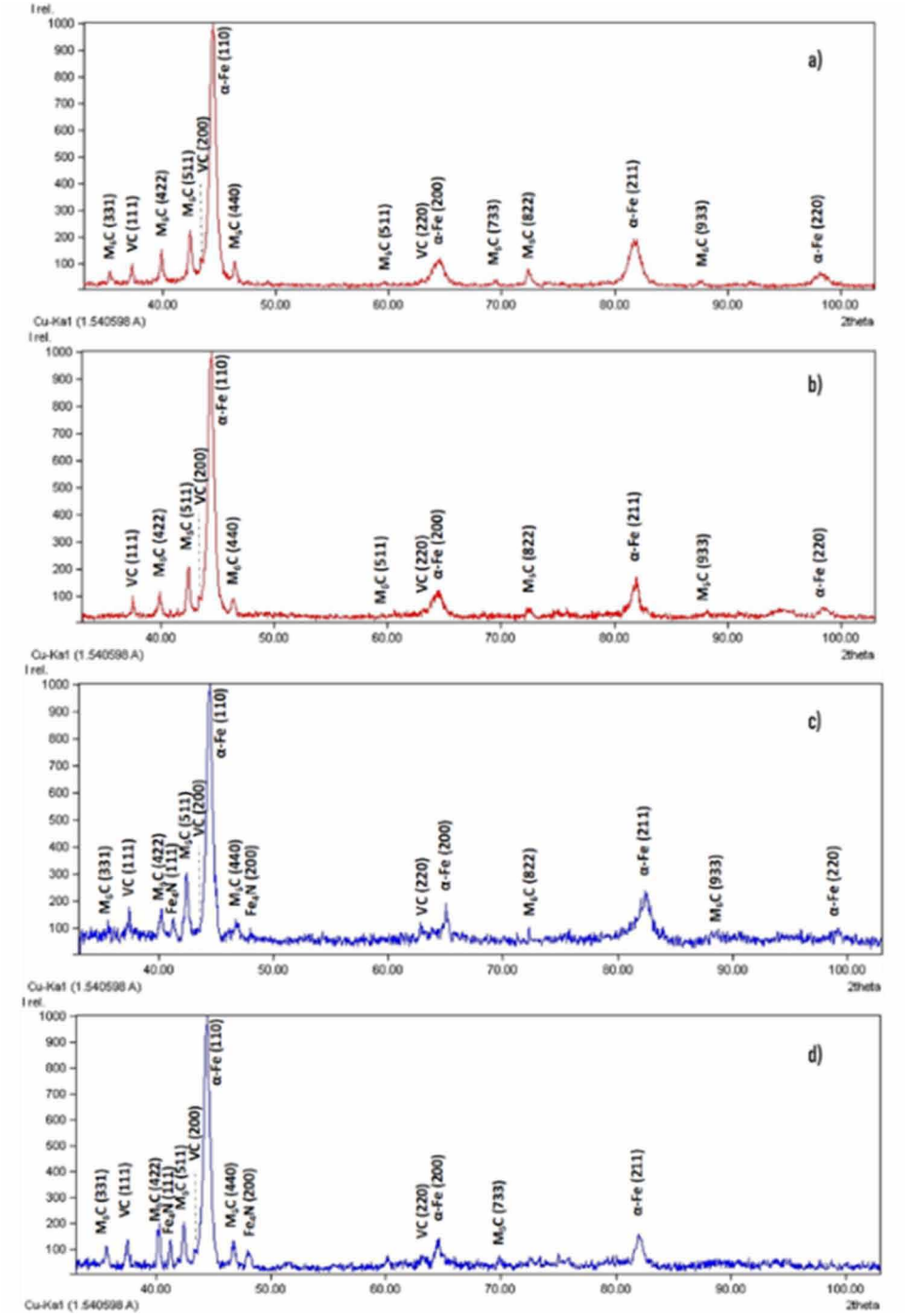

One of the most effective ways to improve the physical and mechanical properties of the surface layer of high-speed steels is the development of optimal nitriding modes. It is practically impossible to choose the necessary nitriding regimes without a detailed study of phase transformations in the material during nitriding.

Figure 14 shows XRD patterns of M2 steel before and after nitriding. XRD analysis show that in the initial state, after standard heat treatment, the M2 steel structure contains martensite (α-phase) and M_6C, MC carbides. After nitriding, broadening, a decrease in intensity, and a shift towards smaller Bragg angles of the interference line (110) of the α-phase are observed. These indicate the formation of a solid solution of nitrogen in iron, i.e., internal nitriding zone (Kuksenova, et al., 2004). On the diffraction patterns of M2 steel samples nitrided at 500°C and 550°C, interference lines of the Fe_4N phase were observed.

After nitriding the martensite structure is more fragmented and characterised by a defective substructure. The resulting imperfection, apparently, approaches the defectiveness of the grain boundaries. The formation of such a substructure of grains during electrolytic-plasma nitriding may be due to the increased energy in the surface and subsurface layers bombarded with ions and neutral atoms of low-temperature plasma during treatment.

More work is needed to study fine structure of steels and its evolution during chemical-thermal treatment, particularly high-speed steels. The formation of secondary phases in the surface layers of high-speed steels during plasma nitriding is of interest.

As noted earlier, the structure of high-speed steel in the initial (heat-treated) state is tempered martensite with hard carbides. XRD analysis established that Fe_4N nitride is formed in the surface layer after nitriding. SEM analysisshowed that after nitriding at 550°C, fine nitrides of alloying elements are formed in the surface of high-speed steel. However, XRD did not show the presence of nitrides of alloying elements, possibly due to the low concentration and shallow depth of their formation (Skakov, Rakhadilov, Karipbayeva et al, 2014; Skakov, Rakhadilov, & Rakhadilov, 2014). Therefore, to reveal the crystal structures of the secondary phases formed during nitriding, the fine structure of M2 steel samples before and after nitriding at 550°C for 7 min were investigated using transmission electron microscopy (TEM).

Previously, X-ray diffraction studies, the results of which are discussed in (Skakov, Rakhadilov, and Sheffler, 2013; Skakov, Rakhadilov, and Karipbayeva, 2013), showed that the structure of M2 steel in the initial state, i.e. after standard heat treatment, consists of α'-phase based on iron with special carbides M6C and MC. The results of TEM studies confirm these data. The fine structure of M2 steel, observed by electron microscopy, is shown in Figure 15. It is clearly seen that the main phase is the α′-phase (martensite) and that carbide particles of globular morphology occupy a significant part of the volume. Morphologically, the carbide phases are more clearly faceted. It should be noted that the α′-phase has a body-centered cubic bcc crystal lattice and can be iron-based solid solutions of interstitial atoms (C, N, B, S, P, etc.) and substitution (Si, Mn, Ni, Cr, Mo, V, W, etc.) at the same time. In the case of the steel under study, the α′-phase is possibly a substitutional solid solution of Cr, W and Mo and an interstitial solid solution of carbon.

After nitriding, the martensite structure is more fragmented and is characterized by a defective substructure. The resulting imperfection, apparently, approaches the defectiveness of the grain boundaries. The possibility of forming such a substructure of grains during electrolytic-plasma nitriding is provided by the increased energy state of the surface and subsurface layers, which are bombarded with ions and neutral atoms of low-temperature plasma throughout the treatment.

Figure 15. Electron microscopic image of the fine structure of M2 steel before (a) and after (b) nitriding at 550^{0}C

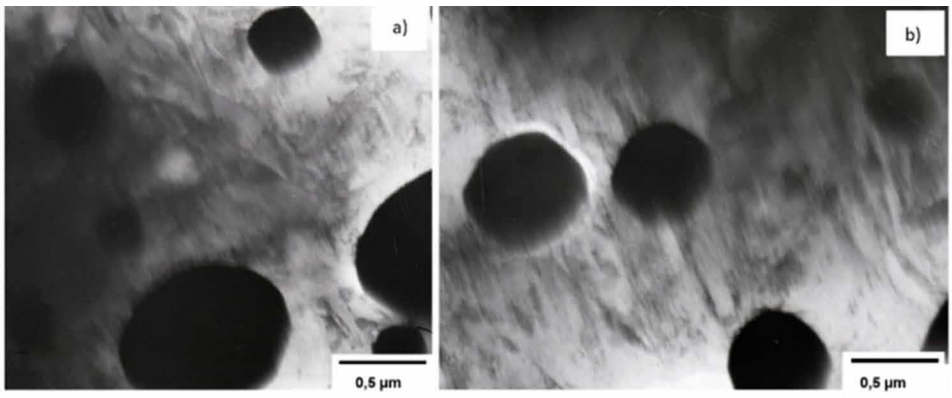

Figure 16. Electron microscopic images of the fine structure of steel M2 before nitriding and their microdiffraction patterns obtained with a matrix (a) and carbides M_6S (b) and MC (c) and schemes for their indexing by Transmission Electron Microscope

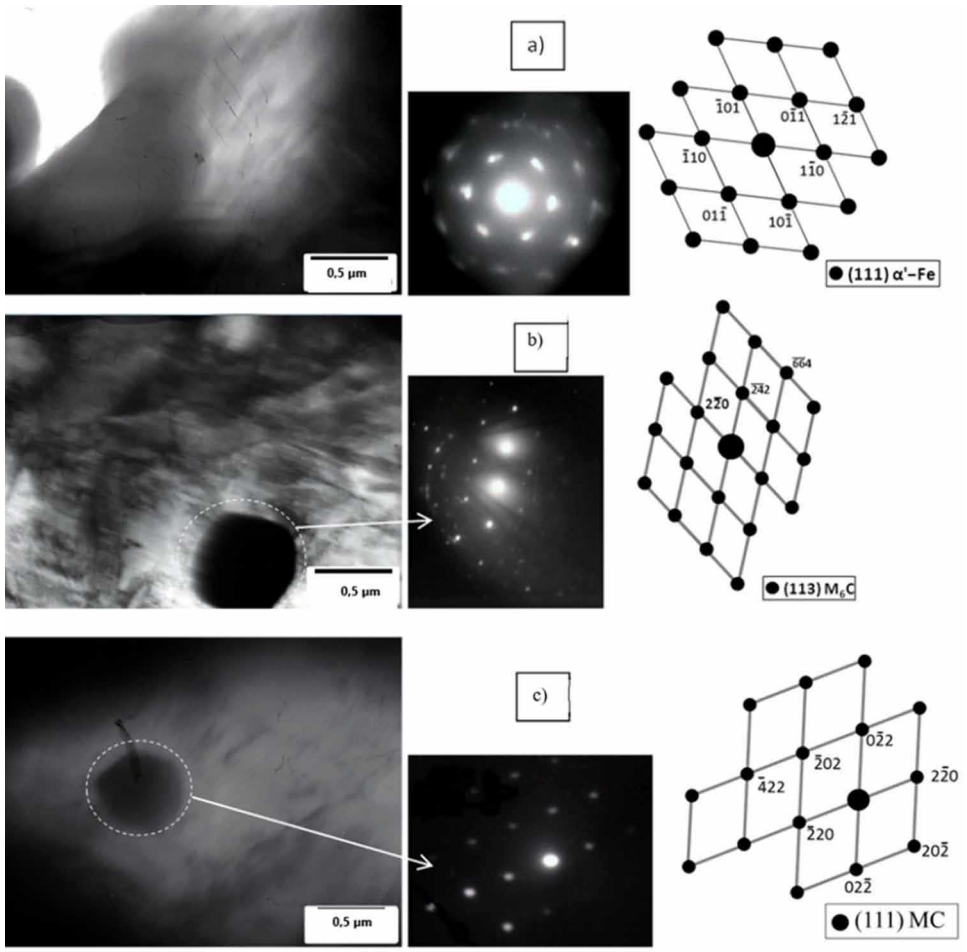

Figure 16 shows TEM images of the fine structure of M2 steel before nitriding and their microdiffraction patterns obtained from the matrix and M_6C and MC carbides and their indexing schemes. Microdiffraction studies have confirmed that the main carbides in steel are M_6C carbide which has a complex FCC crystal lattice and space group Fd3m, and MC carbide, which has an FCC lattice of the NaCl type and space group Fm3m.

Figure 17 shows electron microscopic images of the fine structure of M2 steel after nitriding at 550^0C. After nitriding, particles are formed in the surface layer in the form of thin interlayers (Figure 17 a, indicated by arrows). Finely dispersed precipitates of irregular shape (Figure 17 b, indicated by arrows), randomly located in the martensitic matrix. Thus, the formation of fine precipitates of secondary phases in the surface layer after nitriding was confirmed by the electron microscopic method.

Figure 17. Electron microscopic images of the fine structure of M2 steel after nitriding at 5500C (arrows mark particles of the γ′-phase (a) and fine precipitates of secondary phases (b)) by transmission electron microscope

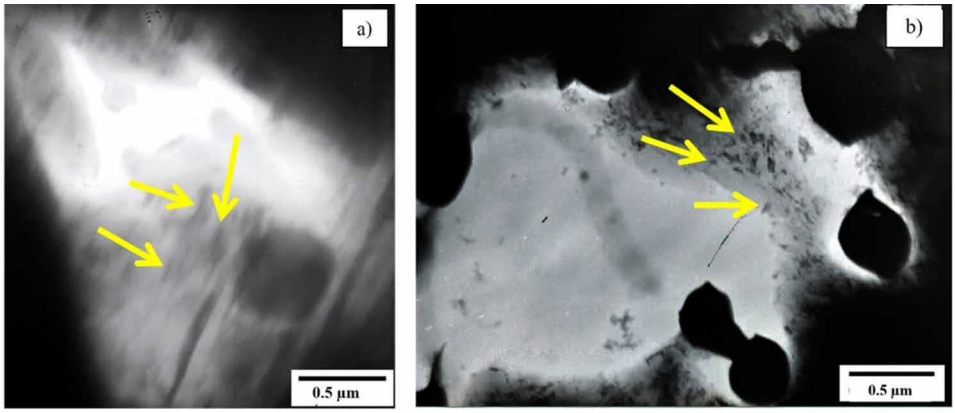

Electron microscopic images of the fine structure of M2 steel after nitriding and their microdiffraction patterns obtained from carbide, matrix and fine nitrides and their indexing schemes are shown in Figure 18.

X-ray diffraction analysis determined that after nitriding at 500 and 550^0C, γ′-nitride is formed in the structure of high-speed steels. From the electron microscopic image obtained from the surface of M2 steel nitrided at 550°C, one can see particles of γ′-nitrides in the form of thin layers. The indexing of the microelectron diffraction pattern shown in Figure 18 showed that the formed thin layers (plate-shaped particles) are iron nitrides of the composition Fe_4N (γ′-phase). Iron nitrides of composition Fe_4N (γ′-phase) are formed upon cooling. Thus, in the process of cooling to room temperature, due to the low solubility of nitrogen in the α-phase at low temperatures, a strongly supersaturated solid solution appears. And this leads to the precipitation, preferably on dislocations, of α′-nitride particles of a lamellar shape with a certain orientation, which are subsequently transformed into γ′-nitrides (Pastukh,, 2006). The mechanism corresponds to the release of carbon and the formation of carbides during the tempering of hardened steel.

Electron microscopic studies have shown that after nitriding, fine precipitates with a size of 50–100 nm are formed on the surface of M2 steel, which are in a nanocrystalline state.

Figure 18. Electron microscopic images of the fine structure of the surface layer of M2 steel formed after nitriding and their microdiffraction patterns obtained from carbide (a), matrix (b) and fine nitrides (c) and schemes for their indexing by transmission electron microscope

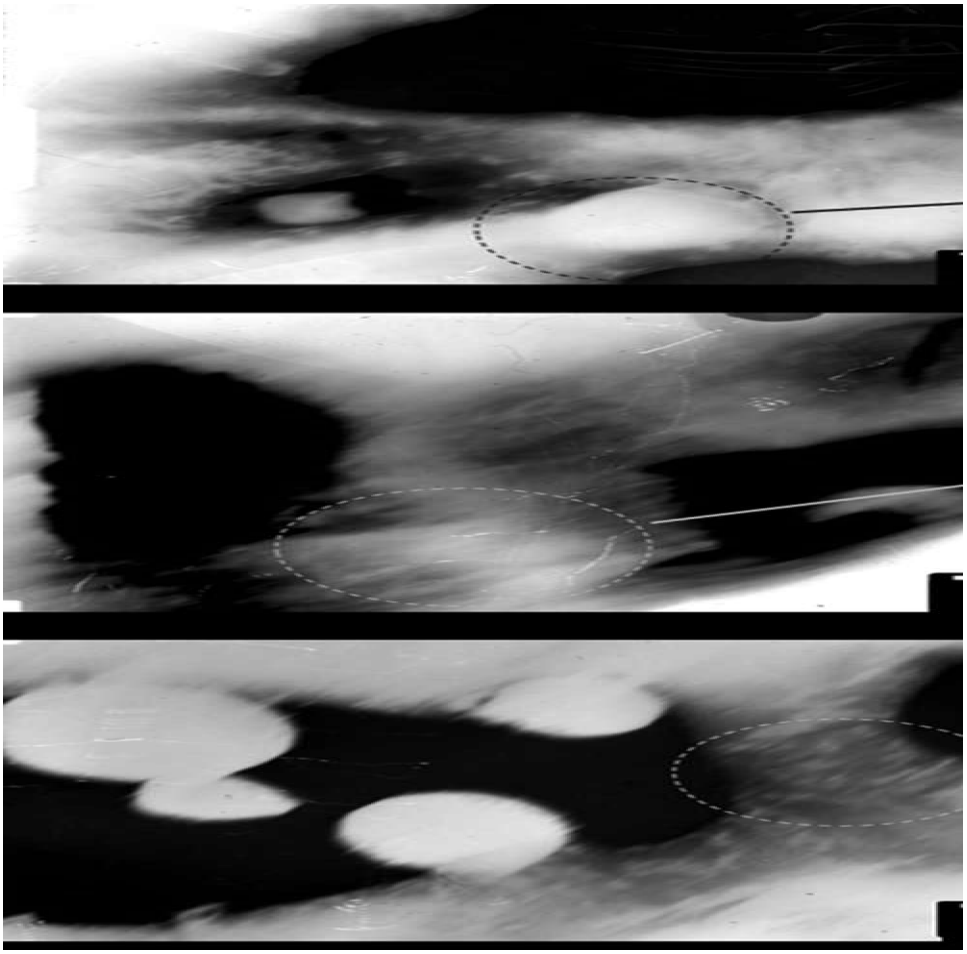

Microdiffraction analysis also showed that the crystal structure of these fine precipitates corresponds to chromium nitride with the composition CrN, which has an FCC lattice of the NaCl type and space group Fm3m. The formation of such CrN nitrides in the surface layers of M2 tool steels after nitriding was observed earlier in (Ramazanov & Vafin, 2011; Shestopalova, 2011). The formation of CrN nitride in high-speed steels is possible in the presence of fluctuations with a sufficiently high concentration (Permyakov, et al., 1972). The presence of concentration fluctuations in solutions in general and in solid solutions in particular is beyond doubt and has been experimentally confirmed in many systems. Under conditions when fluctuations of chromium occur in a medium supersaturated with carbon, they are stabilized at the initial stage due to interaction with carbon (Barabash et al., 1974). This is all the more likely that chromium is a carbide-forming element. Stabilization of fluctuations by carbon creates prerequisites during nitriding for the transformation of the chromium carbon cluster into the nitride phase. The latter is natural in connection with the higher affinity of chromium for nitrogen compared with the affinity for carbon.

Thus, we have characterised all secondary phases formed after nitriding in the surface layers of M2 high-speed steel. These studies are of practical significance because the mechanical properties of high-speed steel are largely determined by the structure and composition of the secondary phases (Gerasimov et al., 2012). It is assumed that the formation of the γ'-phase (Fe_4N) and finely dispersed CrN nitride leads to an increase in the hardness and wear resistance of M2 steel.

CONCLUSION

It has been established that during electrolytic-plasma nitriding of high-speed steels, the process of diffusion saturation of steel with nitrogen occurs with accelerated formation of a modified layer, consisting only of a well-developed zone of internal nitriding, i.e. diffusion layer. It was found that after electrolytic-plasma nitriding at a temperature of 450°C, a modified layer is formed on the surface of high-speed steel, consisting of α′-phase ($Fe_{\alpha(N)}$) and carbides (M_6C and MC), with an increase in the nitriding temperature from 450^0C to 500^0C in the modified layer particles of the γ′-phase (Fe_4N) are formed, and at a nitriding temperature of 550^0C, finely dispersed particles of chromium nitride of composition CrN with an FCC lattice of the NaCl type are formed.

As a result of electrolytic-plasma nitriding at 550°C, a selection of high-speed steels, there was an increase in surface microhardness by 1.6 times. It has been experimentally established that the main increase in the hardness of the diffusion layer occurs after nitriding at 550°C, which is the source of precipitation of finely dispersed nitrides in the supersaturated α-phase, which distort the crystal α-lattice. It has been determined that the important factors influencing the increase in the microhardness of steel is the formation of a diffusion layer from nitrogenous martensite.

It has been established that the main mechanisms that ensure high wear resistance of the nitrided layer of high-speed steels obtained by electrolytic-plasma nitriding are, firstly, the formation of a modified layer consisting only of a diffusion zone (i.e., an internal nitriding zone), and secondly, precipitation in diffusion layer, preferably on dislocations of plate-like γ'-nitrides; thirdly, the formation of fine particles of chromium nitride with the composition CrN in the diffusion layer. It has been determined that the modified layer, consisting of a nitrided α′-phase with a fragmented substructure, M_6C and MC carbides, excess particles of the γ′-phase (Fe_4N) and finely dispersed chromium nitride, obtained after electrolytic-plasma nitriding at 550°C, is wear-resistant, hard, antifriction and has the property of extremely high wear resistance at high temperatures.

The development of engineering technologies in a wide range depends on the technical level of tool production. Thus, one of the problems of environmental protection in mechanical engineering is the high wear resistance of metalworking tools under various conditions of the loading process when machining parts by cutting. Tool life depends not only on the properties of the material, but also on the increase in surface properties. A high role in checking the properties of properties is constantly increasing, which is observed, high efficiency using the methods of chemical-thermal treatment, the scale and development of new areas – engineering of surfaces, methods of energy and physical chemical effects. The implementation of this study when choosing a material significantly improves the performance properties of the tool, as well as reducing the consumption of natural materials. So, in recent applications for calculating emissions and the manifestation of hardening, the increasing use and production of high speed steels, which measures emissions by emissions of hard alloys. An important role in this is played by the use of protection against detection and explosive hardening, which is associated with the use of resource-

saving technologies that help reduce resource costs and increase labor productivity. The most promising method for carrying out methodical hardening is chemical-thermal treatment in an electrolyte plasma, which makes it possible to intensify the saturation process. Reducing the duration of saturation of the process is the subject of close attention to the development of this process.

REFERENCES

Artinger I. (1982). *Instrumental'nye stali i ih termicheskaja obrabotka*, 312.

Barabash R.I., Belobashskiy A.V., & Permyakov V.G. (1974). Tonkaya struktura i uprochneniye azotirovannykh volokon zheleza, legirovannogo khromom. Izvestiya vuzov. *Chernaya metallurgiya,* (10), 118–120.

Erkinbekkyzy, T. E., Zhurerova, L. G., & Daryn, B. (2020). Influence of electrolyte-plasma hardening technological parameters on the structure and properties of banding steel 2. *Key Engineering Materials*, (839), 57–62.

Gerasimov S.A., Kuksenova L.I., & Lapteva V.G. (2012). *Struktura I iznosostoykost' azotirovannykh staley i splavov*, 518. APAN.

Guenzel, R., Matz, W., Ivanov, Yu. F., & Rothtein, V. P. (2000). Pulsed electron-beam treatment of high-speed steel current tools: struchire-phase transformation and wear resistance. *1st International Congress on Radiation Physics, high current electronics, and modification of materials*, (3), 303-307.

Gupta, P., Tenhundfeld, G., Daigle, E. O., & Ryabkov, D. (2007). Electrolytic plasma technology: Science and engineering – an overview. *Surface and Coatings Technology*, *201*(25), 87–96. doi:10.1016/j.surfcoat.2006.11.023

Ivanov, Yu., Matz, W., Rotshtein, V., Gunzel, R., & Shevchenko, N. (2002). Pulsed electronbeams melting of high-speed steel: Structural phase transformations and wear resistance. *Surface and Coatings Technology*, *150*(2-3), 188–198. doi:10.1016/S0257-8972(01)01542-0

Kremnev, L.S. (2008) Teoriya legirovaniya i sozdaniye na yeye osnove teplostoykikh instrumental'nykh staley i splavov optimal'nogo sostava. *Metallovedeniye i termicheskaya obrabotka metallov*, (11),18-28.

Kremnev, L.S. (2008). Teoriya legirovaniya i sozdaniye na yeye osnove teplostoykikh instrumental'nykh staley i splavov optimal'nogo sostava. *Metallovedeniye i termicheskaya obrabotka metallov*, (641), 18-28.

Kuksenova, L.I., Lapteva, V.G., & Berezina, Y.V. (2004). *Struktura i iznosostoykost' azotirovannoystali*, (1), 31-34.

Lakhtin, Y.M. (2009). *Materialovedeniye i termicheskaya obrabotka metallov*, (5),448.

Moiseev, V.F., & Grigor'ev, S.N. (2004). *Instrumental'nye materialy*, 248.

Parfenov, E. V., Yerokhin, A. L., & Mattews, A. (2007). Frequency response studies for the plasma electrolytic oxidation process. *Surface and Coatings Technology*, *201*(21), 8661–8670. doi:10.1016/j.surfcoat.2007.04.044

Pastukh, I.M. (2006). *Teoriya i praktika bezvodorodnogo azotirovaniya v tleyushchem razryade*, 364.

Permyakov, V.G., Belotskiy, A.V., & Barabash, R.I. (1972). Struktura i svoystva diffuzionnoy zony pri azotirovanii khromistogo zheleza. Izvestiya vuzov. *Chernaya metallurgiya*, (4), 129–131.

Petrova L.G. (2001). *Vnutrenneye azotirovaniye zharoprochnykh staley i splavov*, (1), 10-17.

Petrova L.G. (2004). *Vysokotemperaturnoye azotirovaniye zharoprochnykh splavov*, (1),18-24.

Plotnikov, S. V., Pogrebnjak, A. D., Yerokhina, L. N., Yeskermessov, D. K., & Erdybaeva, N. K. (2016). Study of nanostructured (Ti-Zr-Nb)N coatings' physical-mechanical properties obtained by vacuum arc evaporation. *IOP Conference Series: Material Science and Engineering, 110*(1), 1-6. (012031). 10.1088/1757-899X/110/1/012031

Pogrebnjak, A. D., Maksakova, O., Kozak, C., Koltunowicz, T. N., Grankin, S., Bondar, O., Eskermesov, D. K., Drozdenko, A., Petrov, S., & Erdybaeva, N. (2016). *Przegląd Elektrotechniczny*, (8), 180–183.

Ramazanov K. N., & Vafin R. K. (2011). *Razrabotka khorosho ionno-stal'nogo azotirovaniya instrumental'noy KH12 v skreshchennykh elektricheskikh i magnitnykh polyakh*, (41), 101-104.

Shestopalova L.P. (2011). *Issledovaniye khimicheskogo sostava i sostava nitrid-oksidnoy zony oksiazotirovannogo sloya legirovannykh konstruktsionnykh staley,* (54), 78-81.

Skakov, M., Kurbanbekov, S., Tabieva, Y., & Zamanbekuly, E. (2013). Nitriding and carbonitriding influence on stainless steels surface layers changes. *Applied Mechanics and Materials*, *379*, 105–109. doi:10.4028/www.scientific.net/AMM.379.105

Skakov, M. K., Rakhadilov, B. K., & Karipbaeva, G. S. (2013). Specifics of microstructure and phase composition of high-speed steel R6M5. *Applied Mechanics and Materials*, *404*, 20–24. doi:10.4028/www.scientific.net/AMM.404.20

Skakov M.K., Rakhadilov B.K., Karipbayeva G.S., & Manapbayeva A.B. (2014). *Structural-phase state of R6M5 high-speed steel after thermal processing*, (48), 53-59

Skakov M.K., Rakhadilov B.K., & Rakhadilov M.K. (2014). Wear-resistance of nitrided W-Mo-high speed steel in abrasive wear conditions. *Key engineering materials*, (594 – 595).

Skakov, M. K., Rakhadilov, B. K., & Sheffler, M. (2013). Modification of structure and properties of steel R6M5 at electrolyteplasma treatment. *Advanced Materials Research*, (601), 64–68.

Suminov, I.V. (2005). Mikrodugovoye oksidirovaniye teoriya, tekhnologiya oborudovaniye. *EKOMET*, 368.

Vorob'yeva, G.A., & Skladnova, Y.Y. (2003). *Instrumental'nyye materialy: instrumental'nyye stali i splavy,* 100.